Available online at www.sciencedirect.com

ScienceDirect

www.elsevier.com/locate/jmbbm

Research Paper

Ultrasonic assessment of the elastic functional design of component tissues of *Phormium tenax* leaves

*M.D. Fariñas, T.E.G. Álvarez-Arenas**

Sensors and Ultrasonic Technologies Department, Information and Physics Technologies Institute (ITEFI), Spanish National Research Council (CSIC), Serrano 144, 28006 Madrid, Spain

ARTICLE INFO

Article history:
Received 15 April 2014
Received in revised form
6 July 2014
Accepted 17 July 2014
Available online 14 August 2014

Keywords:
Phormium tenax leaf
Functional design
Ultrasound, Vegetal tissues
Tissue mechanical properties
Form and function
Fiber reinforced composites

ABSTRACT

Different tissues in *Phormium tenax* leaves present different morphologies and mechanical properties according to the different roles or functions that they play during the plant life. This is an example of what is known as functional design, a concept which is used in different scientific fields. Four different ultrasonic techniques comprising air-coupling and gel coupling, longitudinal and shear waves, normal and oblique incidence and low (0.2 MHz) and high frequencies (2.25 MHz) have been employed to study these leaves. By changing these experimental conditions it is possible to propagate longitudinal and shear waves in the different tissues present in these leaves (spongy mesophyll, chlorenchyma and sclerenchyma fibres) and in different directions so it is possible to determine their ultrasonic properties (velocity and attenuation) and hence their main elastic mudulii. Additional analysis of microscopic images of the tissues permit to study the correlation between this elastic and ultrasonic tissues properties and main microscopic features like cell size and cell wall thickness, which are determined by the different function of these tissues.

1. Introduction

Functional Design is a concept used in engineering and software and refers to a simplified design approach for complex systems. It is based on the assumptions that the system can be divided into several parts, that each of these parts has only one function and that performs it with the minimum side effects on other parts. It is also used in biology where form and function are inseparable and is applied to the different levels of biological organization (e.g. the morphology of cells, the organization of tissues and the protein design), in the sense that we can often guess how a biological entity works by looking at its structure (Lodish et al., 2000). In addition, functional design space concept is also used in the field of plant evolution (Niklas, 1997).

Phormium tenax, also known as New Zealand Flax is a monocotyledonous plant belonging to the family Agavaceae; its leaves can be up to 3 m long, and contain very long and strong fibers which account for 12–47% of the total cross-sectional area of the leaf, depending on the variety (King and Vincent, 1996). The research and use of these fibers as reinforcement for eco-friendly natural fiber composites is at present going on (e.g. Duchemin et al., 2003; Harris et al., 2005; Cruthers et al., 2006; Le Guen and Newman, 2007;

*Corresponding author.
E-mail addresses: md.farinas@csic.es (M.D. Fariñas), t.gomez@csic.es (T.E.G. Álvarez-Arenas).

http://dx.doi.org/10.1016/j.jmbbm.2014.07.018
1751-6161/

Newman et al., 2007; Wehi and Clarkson, 2014; Duchemin and Staiger, 2009). Different techniques have been used to study the mechanical properties of these fibers, comprising conventional unidirectional stretching tests (De Rosa et al., 2010) and propagation of shock waves (King and Vincent, 1996). Different researches have reported fiber tensile strength in the range 150 to 770 MPa (Jayaraman and Halliwell, 2009; Santulli et al., 2009) and Young's modulus from 10.4 up to 31.4 GPa.

However, not only the fibers but also the whole leaves have been the object of different studies. The presence of these strong fibers provides *P. tenax* leaves the character of a unidirectional fiber reinforced composite, which can be linked to the mechanical functional design of these leaves as it has been done before for grass leaves (Vincent, 1982). Mechanical measurements in different directions in the whole leaf by King and Vincent (1996) have shown a longitudinal and transverse stiffness of 3.98 ± 0.99 GPa and 0.022 ± 0.002 GPa, respectively. Functional design of the cell wall has been studied by a Raman imaging approach by Richter et al. (2011).

Different sonic and ultrasonic techniques has also been employed to the study of plant leaves (Miller,1979; Zebrowski, 1992; King and Vincent, 1996; Fukuhara, 2002; Wilson and Dunton, 2009), though air-coupled ultrasonic techniques in a through transmission configuration has only been recently applied to excite and sense thickness resonances in plant leaves (Álvarez-Arenas et al., 2009a and Fariñas et al., 2013a, 2013b). From the analysis of the magnitude and phase spectra of the first order resonance it is possible to extract the effective mechanical properties of the whole leaf in the direction normal to the leaf plane. Moreover, if a wider frequency spectrum is analyzed and several orders of the thickness resonances are observed, then it is possible to extract mechanical properties of the different layers of tissues that build up the leaf (mainly palisade parenchyma and spongy mesophyll) (Álvarez-Arenas et al., 2009b and Fariñas et al., 2013a, 2013b).

The objective of this paper is to combine different ultrasonic techniques to propagate different types of ultrasonic waves (longitudinal and shear waves with different polarization directions, at different frequencies) and along different directions. Depending on the technique used, the propagation takes place along different paths within the leaf corresponding to different tissues so that it is possible to measure the ultrasound propagation velocities in each of them and hence to work out their mechanical properties. These mechanical properties can be related with other tissues features, obtained from microscopic images, like cell shape, size, cell wall thickness and cell wall volume fraction, which are determined by the function of each of these tissues and cells, e.g. either mechanical support (strong unidirectional fibers), or water transport/storage (parenchyma tissue and sheath cells), or gas interchange (soft spongy mesophyll),.

2. Materials and methods

2.1. Materials

2.1.1. Plant material and preparation

Several *P. tenax* leaves of an unknown cultivar with lengths between 1.2 and 1.8 m were harvested early in the morning. Leaves were then carried to the lab, and all measurements were performed before noon. The basal section of these leaves is folded along the midrib with the upper leaf surface on the inner fold, whereas the distal part is unfolded. The upper leaf surface of the folded part formed an antrum from the basis on, but grew together before the leaf unfolded. Between 5 and 9 points were selected in each leaf along the leaf length in the unfolded leaf portion and all measurements (except those that involve wave propagation along the leaf length) were performed at these points. Once these measurements were finished, circles were excised using a punch holder to measure thickness and density. In addition samples were cut for observation with an optical microscope (see Section 2.2.4). Measurements were repeated several times along the year, in June and September (2013) and January and March (2014).

2.1.2. Ultrasonic equipment

Three pairs of wide band and high sensitivity air-coupled ultrasonic piezoelectric transducers designed and built at CSIC were used. Transducers properties are listed in Table 1.

In addition, for through transmission and direct contact (gel coupling) measurements of longitudinal waves we employed a pair of 1.00 MHz Panametrics transducers (V314), and for ultrasonic propagation along the leaf length we used 0.25 MHz Panametrics transducers (V1012). As coupling medium between transducers and leaves we used the Olympus ultrasonic couplant gel. Commercial Panametrics 2.25 MHz shear wave transducers (V154) were used for shear wave measurements. As coupling medium we used the Panametrics ultrasonic shear couplant gel (SWC).

A Panametrics 5077 pulser/receiver was used for all the ultrasonic measurements. The pulser provides a semicycle of a square voltage signal to drive the transmitter transducer; amplitude of the excitation signal was set to 200 V for air-coupled measurements and to 100 V for the rest of the measurements; pulser frequency was tuned to the transducer centre frequency. Low Pass filter was set off and High Pass filter was set to 10 MHz. The pulser also provides a

Table 1 – Air-coupled transducers properties.

Centre frequency (MHz)	Peak Sensitivity (dB)	Frequency band (MHz)	Radiating surface diameter (mm)
0.25	−25	0.1–0.35	20
0.65	−30	0.35–0.95	15
1.00	−32	0.50–1.30	10

synchronous signal that was used to trigger the oscilloscope. The pulse repetition frequency was set to 200 Hz. Gain at reception was selected to maximize the signal to noise ratio (SNR) without saturating the received signal in the oscilloscope. This was between −10 dB (for gel coupling measurements) and 40 dB for air-coupled measurements.

A Tektronix 7054 DPO 500 MHz digital oscilloscope was used to acquire and digitize the electrical signal generated in the receiver transducer. Samples were averaged 100 times to improve the signal to noise ratio. Vertical resolution is 8 bit, signal length 5 k and sampling frequency 10 MS/s. This is a PC windows based oscilloscope so the oscilloscope has an internal (USB) connection to a PC, digitized signal was stored in the PC for further calculations and analysis

2.1.3. *Other equipment*

A Leica DM 750 microscope fitted with an ICC50 HD camera was used to obtain images of the different tissues and cells in these leaves. An Allmicro microtome was used to get thin layers of the cross section transparent to the microscope. Tissues features shown in the images (like average value and standard deviation of cell diameter, cell wall and solid fraction) were later quantified using imageJ (http://imagej.nih.gov/ij/), a public domain, Java-based image processing program developed by the National Institutes of Health (NIH).

A precision lab balance (Precisa XT220A) were used to weight the circle samples cut out from the leaves, precision is 0.0001 g. Thickness was measured using a micrometer with precision 5 μm.

2.2. *Experimental methods*

Fig. 1 summarized the different leaf and transducers configurations employed for the measurements.

2.2.1. *Measurement of the leaf thickness resonances in the transmission coefficient spectra at normal incidence using through transmitted air-coupled ultrasonic pulses*

Measuring procedure is explained in detail in Álvarez-Arenas (2003a), (2003b). Transmitter (Tx) and receiver (Rx) transducers were mounted facing each other and separated about 5 cm. Leaf is put in between them at normal incidence, as shown in Fig. 1a. The PR 5077 drives the Tx with a 200 V amplitude square semicycle tuned to the transducer centre frequency. Tx launches an ultrasonic pulse to the air that goes through the air gap between Tx and the leaf, then across the leaf, then between the airgap between the leaf and Rx and, eventually, arrives at the Rx; this transducer converts the ultrasonic pulse into an electrical signal that is connected to the PR 5077 where it is amplified and then sent to the 7054 DPO Oscilloscope, where it is digitized, and stored on the PC. A temporal rectangular window is used to filter out the signal reverberations within the air cavities between leaf surface and transducers so that we only get the through transmitted signal. Then, Fast Fourier Transform (FFT) is extracted to obtain magnitude and phase of the transmission coefficient. Measurements were performed in several points (5–7) along the leaf length to check the variability of the leaf properties.

First, measurements were performed around the first order thickness resonance, which was accomplished using the 0.25 MHz pair of transducers. The theoretical analysis of these measurements, assumes that the leaf is a homogeneous plate. Hence, what we really obtained are effective leaf properties. This approach has been applied before for other plant leaves with meaningful results (Álvarez-Arenas et al., 2009a; Sancho-Knapik et al., 2010; Sancho-Knapik et al., 2012).

In a second step, measurements were performed using the other pairs of transducers (see Table 1) to observe higher orders of the leaf thickness resonances. It is known from previous works (Álvarez-Arenas et al., 2009a; Fariñas et al., 2013a, 2013b) that the location of these higher order resonances deviates

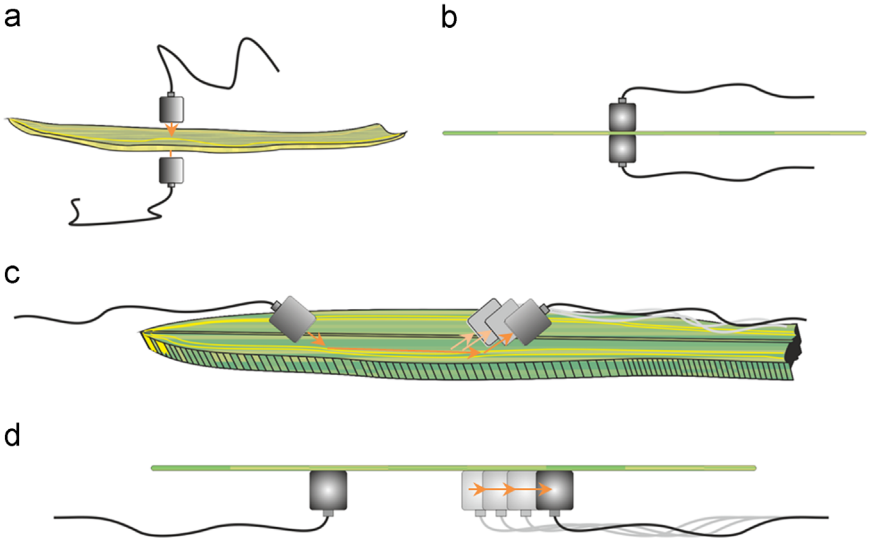

Fig. 1 – Experimental configuration of ultrasonic transducers respect to the leaves: (a), through transmission, air-coupled and normal incidence to excite thickness resonances of longitudinal wave; (b) through transmission, direct contact (gel-coupled) and normal incidence for longitudinal and shear waves; (c), air-coupled and oblique incidence configuration to excite and sense guided waves along the sclerenchyma fibres; (d), gel-coupled configuration for the same purpose as in (c).

from the predictions of the one layer model, and that this is due to layered structure of the leaf in the thickness direction. Therefore using a layered model permit us to get a better fitting of the theoretical calculations into the experimental data, and makes it possible to extract material properties of the different layers of tissue that made up the leaves (Fariñas et al., 2013a, 2013b). Further details of both procedures are given in Section 2.3.

2.2.2. *Measurement of the velocity of longitudinal and shear ultrasonic waves in the leaf thickness direction using gel coupling in through transmission configuration*

Experimental set-up is schematically shown in Fig. 1b. The two V314 Panametrics 1.00 MHz transducers were first attached one directly to the other using gel coupling. Tx was then driven by the PR 5077 and the received signal was stored in the DPO 5074 Oscilloscope. Then, we put the leaf in between the transducers and measure the time delay between this signal and the signal received when both transducers were in direct contact. From this time delay and the leaf thickness measured at the same point using a micrometer, we worked out the ultrasound velocity.

The procedure for the shear wave measurements using the 2.25 MHz shear wave transducers (V154) is similar as the one explained before and Fig. 1b also corresponds to this configuration. In this case, there are two significant differences though. First the gel couplant used in this case is a very viscous one, able to transmit shear waves. The second one refers to the nature of the wave; in this case the transducers generate linearly polarized shear waves, the propagation direction is normal to the leaf plane, and the shear displacement takes place in the leaf plane. As the leaf can be considered as a unidirectional fiber reinforced composite, then there are two different main velocities and we measured both of them; they correspond to the shear waves with the direction of polarization along and normal to the fibres, respectively.

2.2.3. *Measurement of the velocity of ultrasonic waves in the leaf plane along the sclerenchyma fibers direction*

Two different techniques were used for this purpose.

1. Air-coupled 0.25 MHz centre frequency transducers and oblique incidence to generate guided lateral longitudinal waves that propagates along the fibres. Employed technique is the same as used to excite plate waves using the Kremer's rule also called coincidence principle (Cremer., 1947; Brekhovskikh, 1960). Experimental set-up is schematically shown in Fig. 1c. This technique has been widely used in the past to excite Lamb waves in plates and in fiber reinforced polymer plates. The incidence angle of the ultrasonic radiation in the leaf is set so that the projection of the wave length of the incident field coincides with the wave length of the longitudinal waves guided in the fibres, so that a resonant condition is achieved and this mode is generated. The wave propagates along the leaf length and a second transducer facing the leaf at the same angle (but opposite direction) receives the leakage of the wave to the air. This second transducer is displaced along the leaf length in steps of 1.6 mm over a total distance of 100 mm. At each step the received signal is recorded. As the distance between transducers is increased the time delay in the received signal is increased. Time delay is plotted against the distance and it provides a straight line, from the slope of this line we obtain the ultrasound velocity for the propagation in the plane of the leaf.

2. The two gel coupled 0.25 MHz transducers were attached using the coupling gel to the same side of the leaf but separated by a few centimeters. Experimental set-up is schematically shown in Fig. 1d. The Tx is driven as in previous cases and the received signal in Rx is stored. The, Rx transducer is moved away 1 cm, and the process is repeated. The time delay is recorded for each distance and from the graph distance versus time delay we obtain the ultrasound velocity in the leaf plane along the leaf fibers direction. This procedure has also been used in the past to determine velocity of Lamb waves (Szewieczek et al., 2012).

2.2.4. *Other non ultrasonic methods*

Once the ultrasonic measurements were finished, circles were excised from the leaves at the marked points using a punch holder (10 mm diam.). Disk thickness was measured with a micrometer, weighed using the precision balance, and, finally, density was worked out. Then, the excised leaf circles were put in an oven at 80 C for 48 h to remove the water; finally, they were removed from the oven and weighed again to get the dry matter content.

Tissue structure was investigated and photographed for later quantification with a light microscope (Leica DM 750) equipped with a digital camera (ICC50 HD). Two main different kind of observation were performed: (i) cross-section of the leaves at different points along the leaf length (ii) surface of the leaves after removal of the epidermis. Main tissues features like cell diameter, cell wall and/or solid fraction were later quantified using imageJ, a public domain, Java-based image processing program developed by the National Institutes of Health (NIH).

2.3. *Theoretical methods*

2.3.1. *Analysis of the first thickness resonance measured by using air-coupled ultrasound and a through transmission configuration: Effective medium approach*

The measured spectra of the transmission coefficient of different plant leaves in the frequency range limited around the first order thickness resonance can be reproduced by a theoretical model that assumes the leaf as a homogeneous and flat plate and considers normal incidence (Álvarez-Arenas et al., 2009b). In this case a simple analytical expression can be derived for the transmission coefficient (γ), see Eq. (1), that depends on the acoustic impedance of the leaf and the surrounding medium (air in this case): z_1 and z_2, respectively, the thickness of the leaf (t), the ultrasound velocity (c) and the attenuation (α) in the leaf and the ultrasound frequency (f).

$$\gamma = \frac{-2Z_1Z_2}{2Z_1Z_2\cos(kt) + i(Z_1^2 + Z_2^2)\sin(kt)} \tag{1}$$

where $\omega = 2\pi f$, and $k = \omega/c$.

In general, we assume that the attenuation coefficient (α) varies with the frequency (f) following a power law:

$$\alpha = \alpha_0 (f/f_0)^n \quad (2)$$

As the acoustic impedance of a material is the product of the density and the acoustic wave velocity, then γ of a leaf is a function of the frequency of the wave that depends on the following leaf properties: thickness (t), density (ρ), and ultrasound velocity (c) and attenuation (α). All these four leaf parameters can be obtained by fitting the calculated γ according to Eq. (1) into the experimentally measured transmission coefficient spectra (magnitude and phase) without any additional input parameter. A solution of this problem was proposed in Sancho-Knapik et al., 2012, based on a brute force approach. However, we have developed a novel approach that provides better averaged running times. It operates as follows. First, as proposed in Álvarez-Arenas (2010) the measurement of the resonant frequency, the magnitude and the phase of the transmission coefficient at resonance and the Q-factor of the resonance peak are used to get an analytical estimation of the leaf thickness, density, and ultrasound velocity and attenuation coefficient at the resonant frequency. Then, these values are used as initial guess for a fitting routine based on the Gradient Descent method to find the set of leaf parameters (t, ρ, c, α and n) that minimize the error between the calculated transmission coefficient spectra and the measured one. This routine is written in Python 2.7 and is available at the group web page (http://www.us-biomat.com). The ultrasonic estimation of leaf thickness and density are compared with direct measurements obtained with the micrometer and by weighing the circles excised from the leaf with the punch holder. This comparison provides an independent verification of the accuracy of the ultrasonically estimated effective leaf parameters.

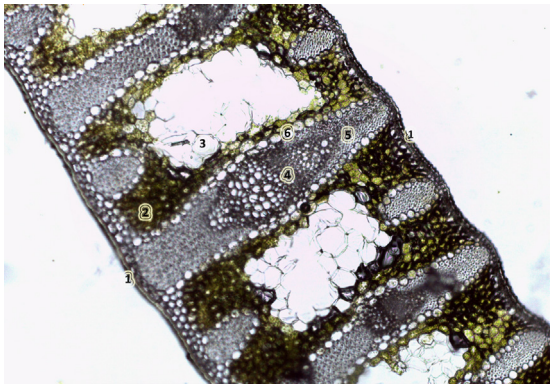

Fig. 2 – Cross-section optical image of a 650 μm *Phormium tenax* leaf at the distal unfolded leaf part: (1) Epidermis; (2) Chlorenchyma; (3) Spongy mesophyll; (4) vascular bundle (xylem and phloem); (5) Sclerenchyma fibres; (6) Bundle sheath.

Table 2 – *Phormium tenax* leaf cross-section structure.

Tissue	Surface ratio (cross-section) (%)
Upper epidermis	6.5±1
Lower epidermis	3.2±1
Sclerenchyma fibers+bundle sheath	26.0±4
Chlorenchyma	36.2±7
Spongy mesophyll	20.1±6
Vascular bundle	8.0±3

2.3.2. *Analysis of the first three thickness resonances measured by using air-coupled ultrasound and a through transmission configuration: Three-layered medium approach*

The solution of the inverse problem case is achieved in a similar way as in the previous case, though in this case, there is no analytical solution for the transmission coefficient as the one shown in Eq. (1). Now the data obtained from the previous step are used as initial guess. Then we assume a layered structure, where, initially, all layers are equal, and we search for the properties of each layer that minimize the deviation between calculated and measured spectra. This search is also performed using a Gradient Descent algorithm. Unlike the previous case, now it is necessary to have some information about the leaf structure in order to reduce the number of parameters and to be able to extract meaningful information. In particular, it is necessary to know: (i) how many layers are necessary to produce a reasonable acoustical representation of the leaf, (ii) the thickness of each layer and (iii) the overall density. The parameters of the multilayered model that are allowed to be changed in the Gradient Descent algorithm are the densities and the ultrasound velocity and attenuation in each of the layers.

The selected acoustical layered model for this case is chosen after the analysis of the leaf cross-section images and is a model that is symmetric respect to the leaf central plane and comprises three layers. Outer layers correspond to epidermis and parenchyma tissues; the central layer comprises the center of the leaf, that is, mainly the spongy mesophyll and the vascular bundle.

2.3.3. *Estimation of elastic moduli from ultrasonic velocity measurements*

For homogeneous and isotropic solids there are simple relations between the elastic moduli, the density (ρ) and the ultrasonic velocities (Auld, 1990). Shear (μ) modulus is directly determined by the shear wave velocity (c_T) according to Eq. (3), in a similar way, the longitudinal wave velocity (c_L) is related to the M elastic modulus (Eq. (4)) which is determined by the bulk modulus K and the shear modulus (Eq. (4)).

$$c_T = \sqrt{\frac{\mu}{\rho}} \quad (3)$$

$$c_L = \sqrt{\frac{M}{\rho}} = \sqrt{\frac{K + 4/3\,\mu}{\rho}} \quad (4)$$

In addition, the velocities ratio: $r = c_T/c_L$ is related to the Poisson's ratio (σ) by Eq. (5):

$$\sigma = \frac{2r^2 - 1}{2(r^2 - 1)} \quad (5)$$

Alternatively, (c_L) can be expressed in terms of the Young modulus (E) and the Poisson's ratio (Eq. (6)).

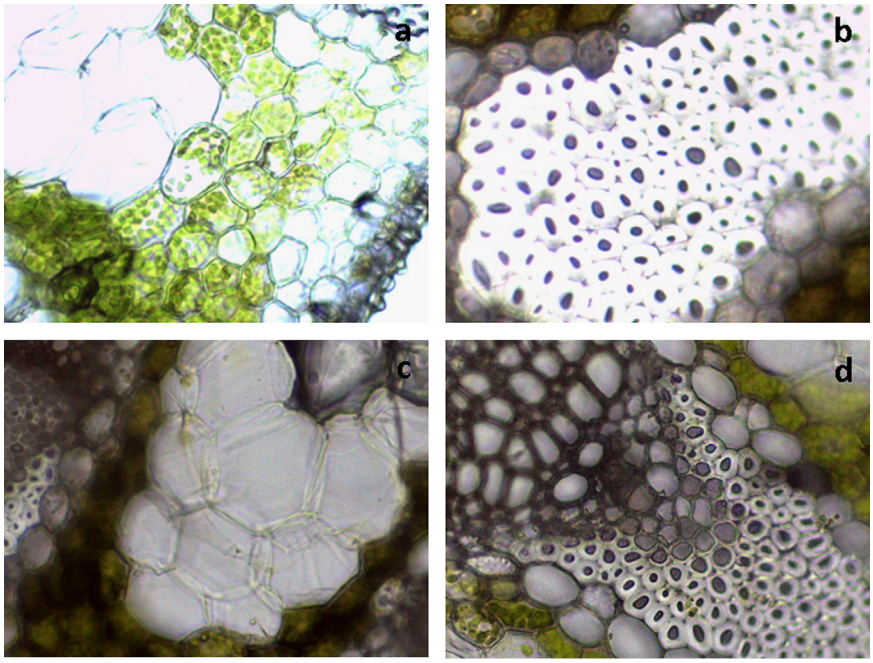

Fig. 3 – Details from *P. tenax* cross-section: (a) Chlorenchyma, chloroplasts are clearly seen (image horizontal width: 160 μm); (b) Sclerenchyma fibres (image horizontal width: 160 μm); (c) Spongy Mesophyll (image horizontal width: 220 μm); (d) Vascular bundle, sheath cells (larger cell without chloroplasts) can be seen surrounding the vascular bundle (image horizontal width: 220 μm).

Table 3 – *P. tenax* cell and cell wall dimensions in the different leaf tissues.

Tissue	Cell diameter (μm)	Cell wall thickness (μm)	Solid fraction ρ^*/ρ_S (%)		
			Eq. (9)	Image	Mean value
Chlorenchyma	26.4±5.6	0.79±0.14	15	25	20
Sclerenchyma	10.67±2.3	3.74±0.77	70	85	77.5
Spongy mesophyll	44.6±24.3	0.35±0.07	5	10	7.5
Bundle sheath	19.2±4.0	1.1±0.15	25	–	25

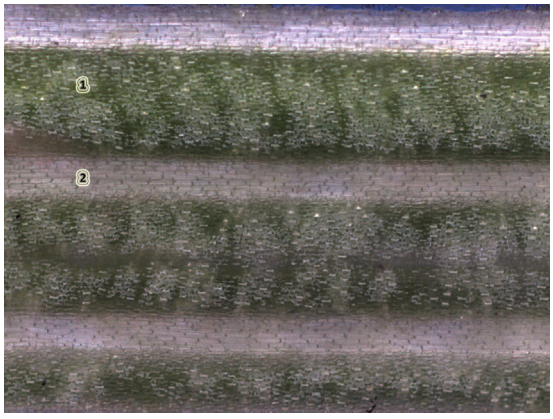

Fig. 4 – Leaf structure in the longitudinal plane below the epidermis: (1) Chlorenchyma tissue (green color is due to the chloroplasts); (2) Sclerenchyma fibres, individual cells (elongated and thick walled) can be seen. (For interpretation of the references to color in this figure legend, the reader is referred to the web version of this article.)

$$c_L = \sqrt{\frac{E(1-\sigma)}{\rho(1+\sigma)(1-2\sigma)}} \tag{6}$$

When material dimensions interfere with the ultrasonic propagation, like in plates or rods, then different relations exist between the elastic constants and the velocities. For example, in the case of plates, it is possible to excite a wide collection of guided waves called Lamb waves. In the particular case of propagation in rods or bars where the wavelength is much larger than the rod diameter, the relationship between the velocity and the Young's modulus is given by:

$$c_{Rod} = \sqrt{\frac{E}{\rho}} \tag{7}$$

For different leaves Poisson's ratio values close to 0.33 has been measured using ultrasonic means (Fariñas et al., 2013a, 2013b), and a value between 0.3 and 0.4 has been estimated by King and Vincent, 1996 to calculate Young modulus values from longitudinal velocity measurements.

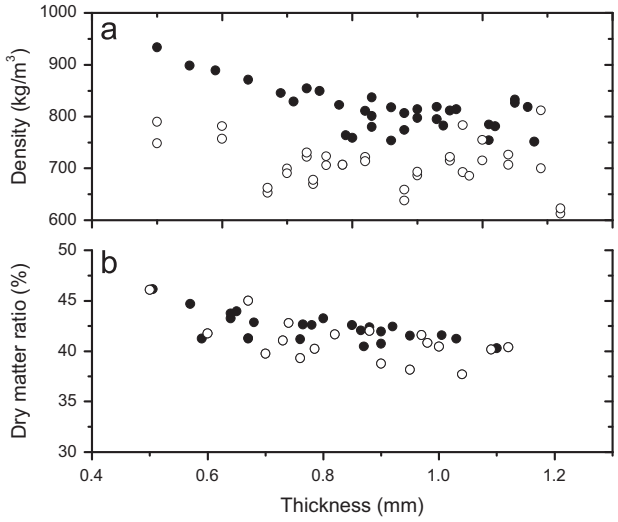

Fig. 5 – Density (a) and dry matter ratio (b) of *P. tenax* leaves in the unfolded leaf section vs. leaf thickness. Black circles: winter *P. tenax* leaves; blank circles: summer *P. tenax* leaves.

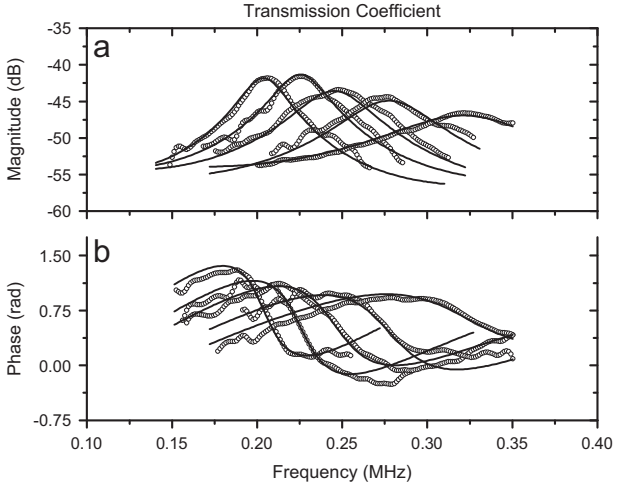

Fig. 6 – Magnitude (a) and phase (b) spectra of transmission coefficient in 5 different points along the length of a *P. tenax* leaf in the unfolded section (thickness: 0.97 mm, 0.85 mm, 0.75 mm, 0.66 mm 0.52 mm); Circles: experimental data; Solid line: theoretically calculated values by the one-layer model.

Finally, assuming that the tissues are closed-cell cellular solids (Gibson and Ashby, 1999), it is possible to estimate the cell wall Young modulus (E_S) from the tissue Young modulus (E^*) and the relative density (ρ^*/ρ_S) according to Eq. (7)

$$\frac{E^*}{E_S} = \left(\frac{\rho^*}{\rho_S}\right)^2 = (1-\varphi)^2 \tag{8}$$

where the superscript $*$ denotes the cellular solid, and the subscript S the solid in the cell wall; $(1-\varphi)$ is the volumetric solid fraction in the tissue. In addition, for closed-cell cellular solids, it is also possible to establish an analytical relationship between the ratio of cell wall length (l) to cell wall thickness (t) and the relative density (ρ^*/ρ_S) (Gibson and Ashby, 1999).

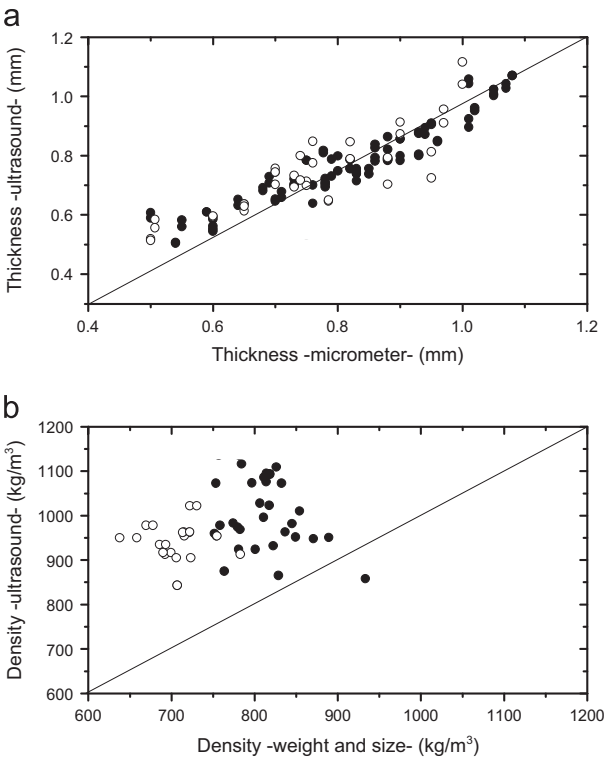

Fig. 7 – (a) Thickness obtained by the ultrasonic technique vs. thickness measured using a micrometer. (b) Density obtained by the ultrasonic technique vs. density obtained from the measured thickness and weight of the excised circles: black circles, values in winter *P. tenax* leaves; blank circles, values in summer *P. tenax* leaves.

$$\rho^*/\rho_S = Ct/l \tag{9}$$

where C depends on cell geometry. For some ideal cases, the value of C can be calculated, for example, it is 1.90 and 1.18 for rhombic dodecahedra and for tetrakaidecahedra cells, respectively.

3. Results

3.1. *Optical microscopy images of the leaf tissues and the cellular structure*

The structure of the *P. tenax* leaf has been the object of previous studies, further details can be seen in King and Vincent, 1996; Richter et al., 2011; and Arévalo et al. (2013). Measurements were taken at the central part of the leaf (unfolded distal part) over a total distance of about 500 mm. Leaf thickness in this area varies typically from 500 μm up to 1100 μm. Fig. 2 shows the typical structure of the studied *P. tenax* leaves. It comprises the adaxial and abaxial epidermis (1), the chlorenchyma (2), the spongy mesophyll (3), the vascular bundle (xylem and phloem) (4), the sclerenchyma fibers (5) and the bundle sheath (6), that is the parenchymatous sheath that surrounds the vascular bundle. Chloroplasts are only present in the parenchyma tissue (2). Mean values

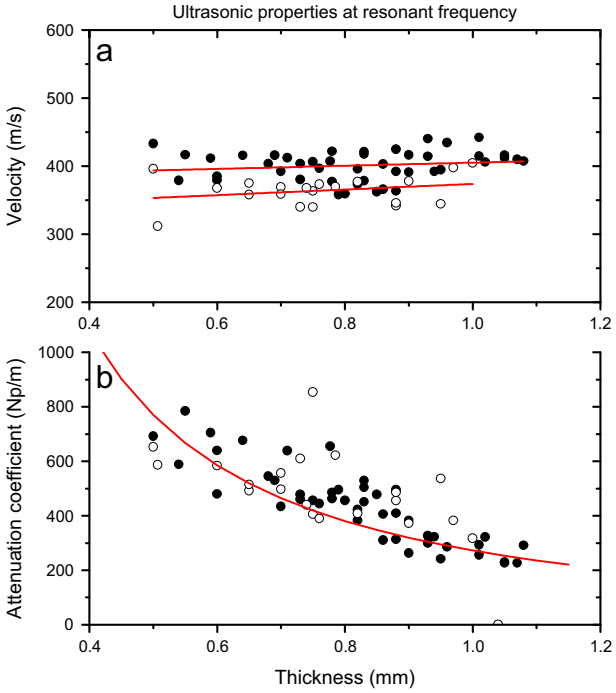

Fig. 8 – Ultrasonic effective parameters of the *P. tenax* leaves obtained from the first order leaf thickness resonance. (a) Ultrasound longitudinal velocity vs. thickness, solid line: linear fitting. (b) Attenuation coefficient at resonant frequency vs. thickness, solid line: power law (Eq. (2) with an exponent of 1.5): black circles: winter *P. tenax*. leaves; blank circles: summer *P. tenax* leaves.

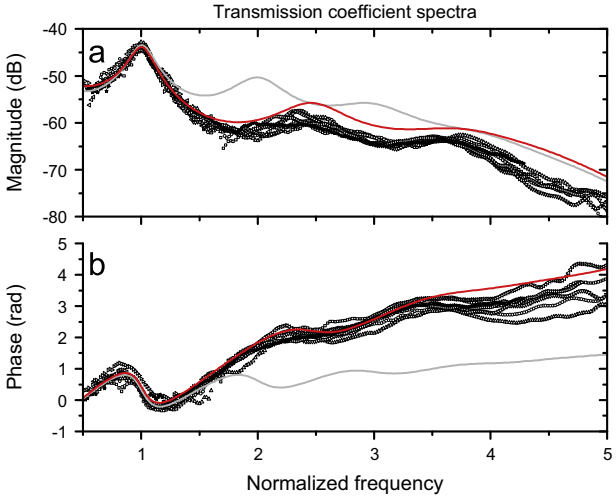

Fig. 9 – Magnitude and phase spectra vs. normalized frequency in seven different thickness points (0.88, 0.85, 0.82 0.78, 0.73, 0.68 and 0.6 mm) for a leaf of *P. tenax* (winter) are shown: Dotted line, experimental data; Solid grey line, theoretical calculations from the one-layer model; Solid red line: theoretical calculations from the three-layers model. (For interpretation of the references to color in this figure legend, the reader is referred to the web version of this article.)

and standard deviation of the surface ratio corresponding to each tissue are shown in Table 2.

The functional design previously mentioned is clearly appreciated in this image. Different sections of the leaf are occupied by different tissues having different morphologies and features that are related with the different functions that these different tissues play in the leaf.

Close-ups of the different tissues revealing the different cellular and tissue structure features that are linked with the different functions of each tissue are shown in Fig. 3. Cell diameter, cell wall thickness and estimated solid fraction from the images and Eq. (9) are summarized in Table 3. Sclerenchyma fibers present the typical thick walled cells which correspond to the primary and the secondary cell walls that provide mechanical support to the plant. These cells are mainly dead, as those in the xylem that also present a thick cell wall but a large inner aperture to allow the flow of water and minerals. Chloroplasts in the mesophyll are clearly seen, they provide the observed dark green color of this tissue.

Fig. 4 shows the leaf structure in the leaf plane just below the epidermis, bands corresponding to the chlorenchyma tissue and the fibers with the elongated sclerenchyma cells are clearly appreciated.

3.2. *Non-ultrasonic measurements: Thickness, dry matter and density*

Measured density vs. thickness and dry matter ratio vs. thickness in the unfolded distal leaf section are shown in Fig. 5. Density in the thinner part of the leaves tends to be larger and this trend is clearer in winter than in summer leaves. In a similar way, dry matter ratio tends to be larger for thinner leaves and is also larger for winter leaves. However, differences are small and the features of the leaves seem to be scaled according to the leaf thickness. Mean and standard deviation density values are $(815 \pm 40)\ kg/m^3$ and $(705 \pm 60)\ kg/m^3$, for winter and summer leaves, respectively.

3.3. *Leaf thickness resonances at normal incidence using air-coupled ultrasound in the vicinity of the first order resonance*

Transducers configuration in this case is the one shown in Fig. 1a. As an example, Fig. 6 shows some of the measured and the calculated magnitude and phase spectra of the transmission coefficient obtained in this case.

As explained before, from the fitting of the theoretically calculated spectra into the experimental data we extract the following leaf parameters: t, ρ, c and α. Fig. 7 shows the plot of the thickness measured using a micrometer vs. the thickness obtained by the ultrasonic technique, and the plot of the density obtained from the measured thickness and weight of the excised circles vs. the density obtained by the ultrasonic technique. Averaged and standard deviation density values are $(995 \pm 85)\ kg/m^3$ and $(956 \pm 70)\ kg/m^3$, for winter and summer leaves, respectively. While the agreement in the thickness estimation between the two techniques is within the dispersion of the measurements, there is a clear bias in the density measurements and the ultrasonically estimated density is always larger that the density value obtained from thickness,

Table 4 – Ultrasonic properties of different tissues of winter and summer *P. tenax* leaves.

Time of year	Tissue	Density (kg/m^3)	Ultrasound velocity (m/s)	Utrasound attenuation (Np/m)	M-elastic modulus (MPa)
Summer	Spongy mesophyll	500±15	450±15	350±10 (@ 250 kHz)	100±7
	Epidermis+chlorenchyma	960±20	560±20		300±20
Winter	Spongy mesophyll	650±15	420±15	365±10 (@ 250 kHz)	115±7
	Epidermis+chlorenchyma	950±20	500±20		240±20

section and weight measurements. This can be explained by the layered structure of the leaf and the relatively larger density of the tissues at the leaf surface (see Section 4).

Ultrasound velocity and attenuation coefficient (measured at the resonant frequency) vs. thickness are shown in Fig. 8 In the case of the velocity results, the solid line represent a linear fitting, for attenuation data, the solid line is, following Eq. (2), a power law fitting (vs. thickness) with an exponent of 1.5. Measured velocities are comparable to the values measured before for leaves of other species. Attenuation values are very large (200–800 Np/m, for frequencies between 200 and 300 kHz), and are also similar to other values found before. This large attenuation coefficient is due to the complex and porous structure of the leaf. Winter leaves present a slightly large velocity values while velocity is rather independent of the thickness, and the attenuation coefficient increases as the thickness decreases. This is due to the fact that measurements at thinner leaf sections are taken at a larger frequency (see Fig. 6), and attenuation increases with the frequency (Eq. (2)).

3.4. *Leaf thickness resonances at normal incidence using air-coupled ultrasound over a wider frequency range (several orders of the thickness resonances)*

The experimental set-up is the same as in the previous case, but now, a larger frequency band is analyzed. As an example of the obtained results, measured and calculated spectra of the transmission coefficient for one leaf at seven different points having different thickness (0.88, 0.85, 0.82 0.78, 0.73, 0.68 and 0.6 mm) are shown in Fig. 9. To get a clearer representation of all these data, magnitude and phase spectra are plotted against the normalized frequency where the frequency of the first order thickness resonance is used to normalize the frequency axis. Gray solid line corresponds to the calculated spectra assuming the leaf as a homogeneous layer and using the parameters obtained in the previous section (Section 3.2). As it has previously been observed for other species (Álvarez-Arenas et al., 2009a and Fariñas et al., 2013a, 2013b), the one layer homogeneous model fails to predict the leaf response outside this narrow frequency window. Red solid line represents the calculated values obtained with the three layers model as explained in Section 2.3. Obtained properties of each of these layers from the fitting of the theoretically calculated transmission coefficient spectra into the experimental data are shown in Table 4.

As expected, spongy mesophyll presents a lower density and a lower velocity. If a Poisson's ratio value of 0.33 (Fariñas et al., 2013a, 2013b) is assumed, then it is possible to obtain the tissue's Young's modulus (Eq. (6)), and with the relative density values in Table 3 it is possible to calculate the cell wall Young's modulus. These estimations appear in Table 5.

3.5. *Through transmission ultrasonic longitudinal and shear wave measurements in the direction normal to the leaf plane using gel coupling*

Measurements were performed with the transducers and leaf configuration shown in Fig. 1b using the 1.00 MHz longitudinal wave transducers and the 2.25 MHz shear wave transducers. In all cases propagation took place in the direction normal to the leaf plane. For the case of the shear wave, measurements for two different polarizations were performed: along the fiber direction and normal to the fiber direction. Results are shown in Fig. 10 for winter leaves. Straight lines represent a linear fitting.

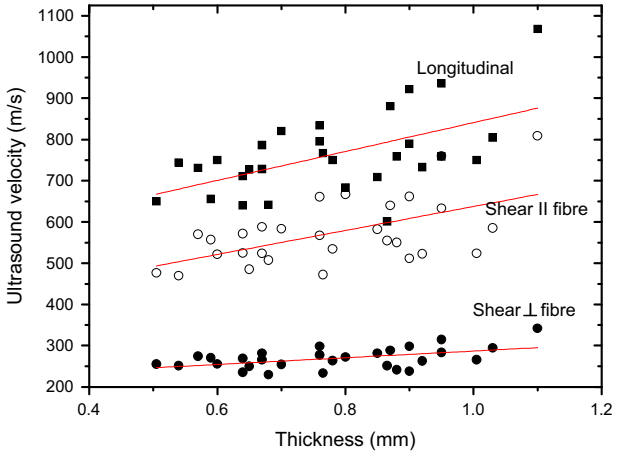

Fig. 10 – Ultrasound velocity measurements for longitudinal and shear waves (both in fibres direction and perpendicular to them) vs. thickness in winter *P. tenax*. leaves: Dot, experimental data; Solid line, linear fitting.

Mean values and standard variation are: (762±98.6) m/s, for the longitudinal wave, and (268.9±25.3) m/s and (572.8±81.2) m/s for the shear waves with polarization in the fiber direction and normal to it, respectively. In this case, longitudinal wave propagation takes place most likely through the fibers and the sheath cells (and this can be the reason for the differences with the longitudinal velocity values presented in previous sections, a further analysis is in Section 4). If we assume a density of 950 kg/m^3, then the M-elastic modulus is 550 MPa, which is a much larger value than those obtained before for the chlorenchyma and the spongy mesophyll. A more detailed analysis of these results in terms of material elastic constants must take into account the composite and anisotropic nature of this tissue.

Table 5 – Estimated Young's modulus.

Time of year	Tissue	Tissue Young's modulus (MPa)	Cell wall Young's modulus (GPa)
Summer	Spongy mesophyll	68.3	12.1
	Epidermis+chlorenchyma	203.2	5.1
Winter	Spongy mesophyll	77.4	13.8
	Epidermis+chlorenchyma	160.3	4.0

Procedures developed to study unidirectional fiber reinforced composites (see, for example, Sinha, 1995) can be applied to this case, this will be the subject of a future work.

3.6. *Ultrasonic propagation along the leaf length*

Measurements were performed with the transducers and leaf configuration shown in Fig. 1c and d. For both cases, propagation took place along the leaf length. For the first case, and as an example of the obtained results, Fig. 11 shows a waterfall of all

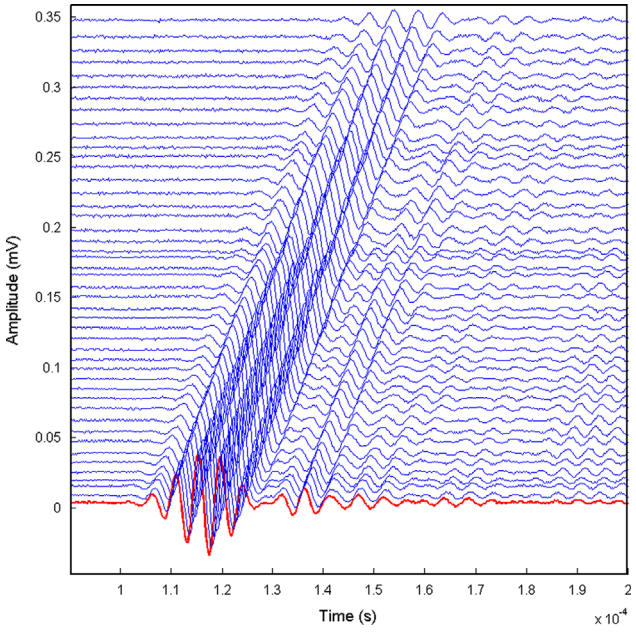

Fig. 11 – Waterfall of the ultrasonic signal propagated along the sclerenchyma fibers of a *P. tenax*. winter leaf.

the received signals as the distance between transmitter and receiver transducer was incrementally changed. Displacement of the receiver transducer is represented as an offset. Measurements were repeated in six different leaves, obtained mean velocity and standard deviation is (2550±250) m/s. In addition, from the amplitude loss of the signal we can calculate the apparent attenuation. This is (25±5) Np/m. Similar measurements were performed with the configuration shown in Fig. 1d. In this case, separation between transducers was set to 5, 10, 15 and 20 cm; measured mean velocity value and standard deviation is: (2670±250) m/s. These results are comparable to those obtained from the study of longitudinal shock wave propagation along the fibers by King and Vincent, 1996: (2354±191) m/s.

Some additional features are of interest. In the first place, and unlike Lamb wave in carbon fiber reinforced composites, measured using the same technique and the same frequency (Fariñas et al., 2012), measurements in *P. tenax* leaves (and shown in Fig. 11) do not present dispersion, in the sense that phase and group velocities are the same. In addition, comparing velocity and attenuation values with those obtained before in the direction normal to the leaf plane we find that attenuation coefficient (25 Np/m) is much smaller and ultrasonic velocity is much larger.

Considering that this propagation takes place along the sclerenchyma fibers, then Young's modulus is given by Eq. (7). Considering a density of the sclerenchyma tissue of 950 kg/m^3, then, the Young's modulus of fibers (in the fiber direction) is 6.76 GPa, and Young's modulus of the cell wall must be about 12 GPa.

4. Discussion

When an ultrasonic pulse arrives at the surface of a *P. tenax* leaf multiple mode conversion processes may take place. Due to the complex *P. tenax* structure, with different tissues that play different functions and have different mechanical properties, there are a number of different propagation modes and propagation paths. The efficiency of the mode conversion phenomena is not equal for all these modes and propagation paths as it is determined by the matching of the acoustic impedance of each of these modes and the acoustic impedance of the medium where the incident wave comes from (either air, or an ultrasonic gel) and other geometric factors like the angle of incidence and the direction of propagation in the leaf. Another factor that determines the possibility to observe or not these modes is the attenuation, and the attenuation depends on the frequency and on tissue features like porosity, presence of other scatterers or inhomogeneities, etc. Therefore changing the coupling technique (either air or gel), the frequency and the incident angle it is possible to change the mode conversion balance so that different modes are preferentially generated and/or detected.

This can explain the different values of the longitudinal wave velocity in the thickness direction measured with the air-coupled and the gel coupling techniques: by changing the interface conditions we are changing the mode conversion balance and we get ultrasonic waves that propagates along different paths. In the first case (between 350 and 450 m/s), the propagation takes place mainly through the chlorenchyma and the spongy mesophyll and, in the second case (between 600 and 900 m/s), through the sheath cells and the sclerenchyma fibers. In addition, the frequency of the gel coupling transducers is higher (1.00 MHz) than the frequency of the first order thickness resonance (between 200 and 300 kHz). It is expected a very large attenuation in the soft

and porous spongy mesophyll tissue that would impede the ultrasonic propagation along this section of the leaf at the higher frequencies.

In a similar way it is possible to explain the large differences observed for propagation in the leaf plane (along the fibers) and in the direction normal to the plane. Propagation in the leaf plane takes place mainly along the fibers, in addition, in this case, large propagation paths are studied (up to 10 mm) which eliminates the possibility to observe the wave that propagates along the chlorenchyma, as it present a larger attenuation coefficient.

Measured density using the first order thickness resonance and the one layer model provides biased density estimation towards larger density values. The main reason is the simplification of the one layer model compared with the actual leaf structure. Actually, the layered model and the measurements over a wider frequency range provide an accurate estimation of the overall density. Two reasons can be given to explain this behavior of the one layer model. In the first place, we have to consider that what the model really obtains from the measured spectra are the velocity of ultrasound and the acoustic impedance of the leaf; hence, density is worked out. The difference between the acoustic impedance of the material (leaf) and the surrounding fluid (air) determines, the amount of energy that is transmitted and reflected at the leaf surface. However, density at the leaf surface (epidermis+chlorenchyma) is expected to be larger than the density in the inner part of the leaf (spongy mesophyll), therefore, if we estimate leaf density from impedance measurements, it is expected to get a biased result. In addition, there must be some internal reflections in the leaf at the interface between the chlorenchyma and the spongy mesophyll, however, the one layer model cannot properly account for this loss of energy and assumes that this is produced at the leaf interface by wrongly estimating a larger leaf density.

Finally, it is remarkable the fact that tissues with extremely different Young modulus are present in these leaves which can be understand as a manifestation of the functional design concept. These differences are consistent with the different functions of the different tissues and the differentiated cellular structure. For example, Young modulus varies from close to 7 GPa for fibres in the fiber direction down to values close to 70 MPa for the spongy mesophyll. On the other hand, observed variations in the cell wall Young modulus are comparatively smaller (from 4 to 5 GPa for chlorenchyma cells, to 12 GPa for sclerenchyma fibers). This reveals the fact the differences in the elastic properties of the different tissues, that are required by their different functions, are mainly furnished by changing the cell form and shape.

5. Conclusions

Different ultrasonic properties (velocity and attenuation) can be measured in *P. tenax* leaves by changing the angle of incidence, the coupling conditions, the frequency and the type of incident wave used. Elastic moduli can be calculated from these velocity data. With the aid of microscopic images, these different results are explained by considering that different kind of ultrasonic waves are excited depending on the experimental set-up. For example, air-coupled and thickness resonance methods are well suited to excite ultrasonic waves in the leaf section that comprises the chlorenchyma and the spongy mesophyll, while by putting the transducers directly in contact with the leaf with the aid of a coupling gel we, preferentially, excite waves in the sclerenchyma fibres and the sheath cells. On the other hand, using oblique incidence, air-coupling and the coincidence principle it is possible to excite guided waves along the sclerenchyma fibers. Elastic constants of these different tissues cover a wide range, and this variation is linked to the different functions of the different tissues, so these ultrasonic techniques can be used to assess the mechanical functional design of the tissues of these leaves. Sclerenchyma fibers do provide mechanical support, consequently, they are more rigid and this is achieved by a very thick cell wall, on the contrary, spongy meshophyll cells mainly store water and interchange it and constitutes a much softer tissue, which is accomplished by large and thin-walled cells, that can be easily deformed to accommodate to the variations in the leaf water content, Finally sheath cells seems to be, from the mechanical point of view, a transition layer to efficiently connect the soft spongy mesophyll and the hard vascular bundle and to ensure leaf mechanical integrity in spite of the large deformations that can take place in the leaf produced during water content fluctuations.

The presented combination of ultrasonic techniques and image analysis have the potential to be applied to other similar cases to assess the mechanical properties of different tissues with different functions and to correlate both features.

Acknowledgements

Funding by Spanish Government, project DPI 2011-22438 is acknowledged. Authors also acknowledge helpful suggestions by L. Gibson and K.J. Niklas and discussions with J.L.F Vincent.

REFERENCES

Álvarez-Arenas, T.E.G., 2003a. Air-coupled ultrasonic spectroscopy for the study of membrane filters. J. Membr. Sci. 213, 195–207.

Álvarez-Arenas, T.E.G., 2003b. A nondestructive integrity test for membrane filters based on air-coupled ultrasonic spectroscopy. IEEE Trans. Ultrason. Ferroelectr. Freq. Control 50 (6), 676–685.

Álvarez-Arenas, T.E.G., Sancho-Knapik, D., Peguero-Pina, J.J., Gil-Pelegrín, E., 2009a. Noncontact and noninvasive study of plant leaves using air-coupled ultrasounds. Appl. Phys. Lett. 95 (19), 193702.

Álvarez-Arenas, T.E.G., Sancho-Knapik, D., Peguero-Pina, J.J., Gil Pelegrin, E., 2009b. Determination of plant leaves water status using air-coupled ultrasounds. In: IEEE Int. Ultrason. Symp., 771–774.

Álvarez-Arenas, T.E.G., 2010. Simultaneous determination of the ultrasound velocity and the thickness of solid plates from the analysis of thickness resonances using air-coupled ultrasound. Ultrasonics 50 (2), 104–109.

Arévalo, C.A., Castillo, B., Londoño, M.T., 2013. Mechanical properties of rosemary (*Rosmarinus officinalis* L.) stalks. Postharvest Biol. Technol. 31 (2), 201–207.
Auld, B.A., 1990. Acoustic Fields and Waves in Solids, second ed. Krieger Publishing Company (June).
Brekhovskikh, L.M., 1960. Waves in Layered Media. Academic Press.
Cremer., L., 1947. Über die Analogie zwischen Einfalsswinkel und Frequenzproblemen. Arch. Electr. Übertragung 1, 28.
Cruthers, N.M., Carr, D.J., Laing, R.M., Niven., B.E., 2006. Structural differences among fibers from six cultivars of Harakeke (*Phormium tenax*, New Zealand flax). Text. Res. J. 76, 601–606.
De Rosa, I.M., Kenny, J.M., Puglia, D., Santulli, C., Sarasini, F., 2010. Tensile behavior of New Zealand flax (*Phormium tenax*) fibers. J. Reinf. Plast. Compos. 29 (23), 3450–3454.
Duchemin, B., Van Luijk, K., Staiger, M., 2003. New Zealand Flax (*Phormium tenax*) reinforced eco-composites. Ecocomp 2, 1–6.
Duchemin, B., Staiger, M.P., 2009. Treatment of Harakeke fiber for biocomposites. J. Appl. Polym. Sci. 112 (1), 2710–2715.
Fariñas, M.D., Sancho-Knapik, D., Peguero-Pina, J.J., Gil-Pelegrín, E., Álvarez-Arenas, T.E.G., 2013a. Shear waves in vegetal tissues at ultrasonic frequencies. Appl. Phys. Lett. 102 (10), 103702.
Fariñas, M.D., Álvarez-Arenas, T.E.G., Sancho-Knapik, D., Peguero-Pina, J.J., Gil-Pelegrín, E., 2012. Shear waves in plant leaves at ultrasonic frequencies : shear properties of vegetal tissues. In: IEEE International Ultrasonics Symposium.
Fariñas, M.D., Sancho-Knapik, D., Peguero-Pina, J.J., Gil-Pelegrín, E., Álvarez-Arenas, T.E.G., 2013b. Shear waves in vegetal tissues at ultrasonic frequencies. Appl. Phys. Lett. 102 (10), 103702.
Fukuhara, M., 2002. Acoustic characteristics of botanical leaves using ultrasonic transmission waves. Plant Sci. 162, 521–528.
Gibson, L.J., Ashby., M.F., 1999. Cellular Solids: Structure and Properties. Cambridge university press.
Harris, W., Scheele, S.M., Brown, C.E., Sedcole, J.R., 2005. Ethnobotanical study of growth of Phormium varieties used for traditional Maori weaving. N. Z. J. Bot. 43 (1), 83–118.
Jayaraman, K., Halliwell, R., 2009. Harakeke (*Phormium tenax*) fibre–waste plastics blend composites processed by screwless extrusion. Composites Part B 40 (7), 645–649.
King, M.J., Vincent, J.F.V., 1996. Static and dynamic fracture properties of the leaf of tenax (Phormiaceae: Monocotyledones). Proc. R. Soc. London, Ser. B 263 (1370), 521–527.
Le Guen, M.J., Newman, R.H., 2007. Pulped *Phormium tenax* leaf fibres as reinforcement for epoxy composites. Composites Part A 38 (10), 2109–2115.
Lodish, H., Berk, A., Zipursky, S.L., et al., 2000. Molecular Cell Biology, fourth ed. W. H. Freeman, New York (Section 3.3, Functional Design of Proteins).
Miller, D.L., 1979. A cylindrical-bubble model for the response of plant-tissue gas bodies to ultrasound. J. Acoust. Soc. Am. 65 (5), 1313–1321.
Newman, R.H., Clauss, E.C., Carpenter, J.E.P., Thumm, A., 2007. Epoxy composites reinforced with deacetylated *Phormium tenax* leaf fibres. Composites Part A 38 (10), 2164–2170.
Niklas, K.J., 1997. The Evolutionary Biology of Plants. University of Chicago Press, Chicago.
Richter, S., Müssig, J., Gierlinger, N., 2011. Functional plant cell wall design revealed by the Raman imaging approach. Planta 233 (4), 763–772.
Sancho-Knapik, D., Álvarez-Arenas, T.E.G., Peguero-Pina, J.J., Gil-Pelegrín, E., 2010. Air-coupled broadband ultrasonic spectroscopy as a new non-invasive and non-contact method for the determination of leaf water status. J. Exp. Bot. 61 (5), 1385–1391.
Sancho-Knapik, D., Calás, H., Peguero-Pina, J.J., Ramos Fernandez, A., Gil-Pelegrín, E., Álvarez-Arenas, T.E.G., 2012. Air-coupled ultrasonic resonant spectroscopy for the study of the relationship between plant leaves elasticity and their water content. IEEE Trans. Ultrason. Ferroelectr. Freq. Control 59 (2), 319–325.
Santulli, C., Jeronimidis, G., De Rosa, I.M., Sarasini, F., 2009. Mechanical and falling weight impact properties of unidirectional phormium fibre/epoxy laminates. eXPRESS Polym. Lett. 3 (10), 650–656.
Sinha P.K., Composite Materials and Structures, 1995. Published by Published by: composite Centre of Excellence, AR & DB, Department of Aerospace Engineering, I.I.T. Kharagpur.
Szewieczek A., C. Heinze, W. Hillger, D. Schmidt, M. Sinapius, Analysis methods of lamb wave propagation in complex composites. In: The Sixth European Workshop on Structural Health Monitoring, 2012, pp. 1–8.
Vincent, J.F.V., 1982. The mechanical design of grass. J. Mater. Sci. 17, 856–860.
Wehi, P.M., Clarkson, B.D., 2014. Biological flora of New Zealand 10. *Phormium tenax*, harakeke, New Zealand flax. N. Z. J. Bot. 45 (4), 521–544.
Wilson, P.S., Dunton, K.H., 2009. Laboratory investigation of the acoustic response of seagrass tissue in the frequency band 0.5–2.5 kHz. J. Acoust. Soc. Am. 125 (4), 1951–1959.
Zebrowski, J., 1992. Complementary patterns of stiffness in stem and leaf sheaths of Triticale. Planta 187 (3), 301–305.